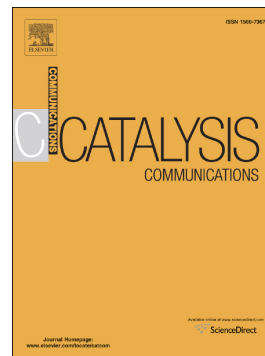


Journal Pre-proof

Direct conversion of ethylene to propylene over Ni- and W-based catalysts: An unprecedented behaviour

Rémi Beucher, Claudia Cammarano, Enrique Rodríguez-Castellón, Vasile Hulea



PII: S1566-7367(20)30167-9

DOI: <https://doi.org/10.1016/j.catcom.2020.106091>

Reference: CATCOM 106091

To appear in: *Catalysis Communications*

Received date: 8 May 2020

Revised date: 15 June 2020

Accepted date: 17 June 2020

Please cite this article as: R. Beucher, C. Cammarano, E. Rodríguez-Castellón, et al., Direct conversion of ethylene to propylene over Ni- and W-based catalysts: An unprecedented behaviour, *Catalysis Communications* (2020), <https://doi.org/10.1016/j.catcom.2020.106091>

This is a PDF file of an article that has undergone enhancements after acceptance, such as the addition of a cover page and metadata, and formatting for readability, but it is not yet the definitive version of record. This version will undergo additional copyediting, typesetting and review before it is published in its final form, but we are providing this version to give early visibility of the article. Please note that, during the production process, errors may be discovered which could affect the content, and all legal disclaimers that apply to the journal pertain.

© 2020 Published by Elsevier.

Direct conversion of ethylene to propylene over Ni- and W-based catalysts: An unprecedented behaviour

Rémi Beucher^a, Claudia Cammarano^a, Enrique Rodríguez-Castellón^b, Vasile Hulea^{a,*}
vasile.hulea@enscm.fr

^aInstitut Charles Gerhardt Montpellier, UMR 5253, ICGM, CNRS, Univ Montpellier, ENSCM, Matériaux Avancés pour la Catalyse et la Santé, 34296 Montpellier, France

^bDepartamento de Química Inorgánica, Facultad de Ciencias, Universidad de Málaga, 29071 Málaga, Spain

*Corresponding author.

Abstract

A new ethylene to propylene catalytic process based on cascade reactions, with two catalysts and two reactors, has been explored in this study. In the first reactor loaded with Ni-ALKIT-6 catalyst, at 60-120 °C and 3 MPa, part of ethylene has been selectively transformed into 2-butene. In the second reactor, loaded with WO_x/KIT-6 catalyst, 2-butene reacted with the unconverted ethylene at 450 °C and 0.1 MPa. Unprecedented results in terms of catalytic activity, selectivity towards the formation of propylene and stability against deactivation were achieved under these conditions. More precisely, an ethylene conversion of ~85% and a selectivity to propylene of 35% and butenes of 30% remained unchanged during 24 h on reaction stream.

Keywords: Tandem catalysis; Heterogeneous catalysis; Metathesis; Ethylene; Propylene; KIT-6.

1. Introduction

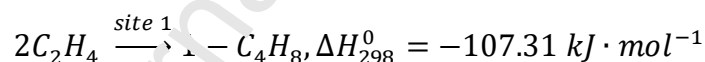
Propylene, a major chemical intermediate, is usually produced from fossil-based feedstock, using highly efficient processes, such as fluidized catalytic cracking and steam cracking of saturated hydrocarbons. Owing to the strong demand for polypropylene during the last years (average annual demand growth of 4.5%), the supply of propylene is of great concern because the traditional sources will not be sufficient to cover the demand. Research efforts have been made to develop alternative routes to propylene production based on accessible raw materials,

such as propane, ca. propane dehydrogenation [1], methanol, ca. methanol to olefins process [2], and ethylene.

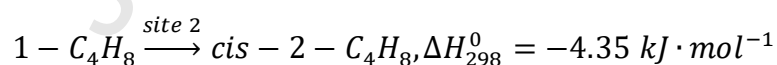
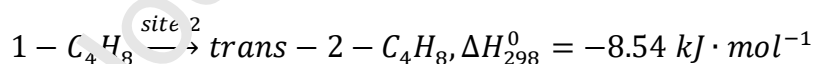
One of the most exciting methods is the conversion of ethylene to propylene (ETP) without the addition of other hydrocarbons [3-6]. The sustainability of this technology is guaranteed by the fact that the ethylene production by dehydration of bioethanol has become economically feasible [7-9]. The ETP process consists of catalytic cascade reactions, including either (a) oligomerization/cracking or (b) dimerization/isomerization/metathesis chemical steps. Typically, oligomerization/cracking is catalyzed by acidic microporous materials like zeolites and SAPOs [10-12] or by multifunctional Ni-mesoporous materials [13-16], at temperatures higher than 350 °C. Generally, mixtures of saturated and unsaturated hydrocarbons of low selectivity to propylene, were produced in such ETP processes.

The processes based on the dimerization/isomerization/metathesis chemical steps are operated at lower temperature (50-150 °C) in the presence of transition metal-based catalysts [17-23]. Three consecutive reactions and three catalytic sites are involved in these processes: (i) dimerization of ethylene to 1-butene, (ii) isomerization of 1-butene to 2-butene, and (iii) metathesis reaction of 2-butene with unreacted ethylene to propylene, as described below.

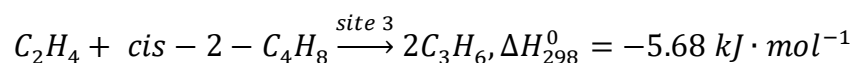
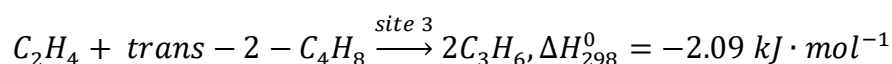
(i) Ethylene dimerization



(ii) 1-Butene isomerization



(iii) Ethylene-butene metathesis



As shown in several studies [17-20], the catalytic sites involved in these reactions could coexist on a single support. Basset and co-workers [17] used a trifunctional WH_3/Al_2O_3 catalyst at 150 °C and 0.1 MPa for the above processes. Li et al. [18] used a single bimetallic supported catalyst, $NiSO_4/Re_2O_7/\gamma-Al_2O_3$ in an ETP process operated at 50 °C and 0.1 MPa. Catalysts like

$\text{MeO}/\text{Re}_2\text{O}_7/\text{B}_2\text{O}_3\text{-Al}_2\text{O}_3$ (Me = Pd or Ni) have been also designated by Buluchevskii et al. [19] for the one-stage ETP process performed at 80 °C and 0.1-1 MPa. More recently, Ghashghaee and Farzaneh [20] developed a nanostructured $\text{Ru-Ba-K-MgO-Al}_2\text{O}_3$ catalyst able to convert ethylene into propylene and butenes at 70 °C and 0.1 MPa. These studies showed that using a single catalyst, which provides different active sites, is a challenging concept. In practice, it is very difficult to balance the catalytic functions involved in the ETP process. Consequently, over these catalysts undesired reactions could occur, causing a decrease in propylene selectivity. Additionally, the catalysts rapidly deactivated.

These weaknesses could be circumvented by distributing the different catalytic sites on two catalysts. Our group developed an original ETP process based on two robust and highly active solid catalysts [21, 22]. In a single reactor operated at 80 °C and 3 MPa, ethylene was first converted over a Ni- AlSBA-15 catalyst into 2-butenes, which then reacted with the unconverted ethylene over a $\text{MoO}_3\text{-SiO}_2\text{-Al}_2\text{O}_3$ catalyst to produce propylene. More recently, we proposed a new efficient heterogeneous catalytic system associating Ni- AlKIT-6 and $\text{ReO}_x/\gamma\text{-Al}_2\text{O}_3$ [23, 24]. Under identical mild conditions (60 °C, 3 MPa), ethylene was very selectively converted into high added value molecules, i.e. propylene and 1-butene. Despite their remarkable initial performance (the initial ethylene conversion was higher than 70%), the supported MoO_x and ReO_x catalysts suffered from significant deactivation after 5 h on reaction stream. Working at low temperature, the loss of catalytic activity was most probably due to the poisoning of active centers by strongly adsorbed products.

Beside the Re- and Mo-based catalysts, W-supported oxides are also well-known metathesis catalysts [25]. It should be noted that a WO_x/SiO_2 catalyst is used in industrial metathesis processes for converting ethylene and 2-butene to propylene [26]. While ReO_x and MoO_x catalysts operate at low temperatures, i.e. 20-80 °C or 80-250 °C, WO_x catalyst is active only at temperatures higher than 400 °C. The long catalyst lifetime compared to MoO_x or ReO_x , the easy and efficient regeneration and the resiliency to oxygenate molecules in the feed are the major advantages of supported WO_x catalysts [27].

In the present study, we prepared and characterized two mesoporous functionalized materials, i.e. Ni- AlKIT-6 and $\text{WO}_x/\text{KIT-6}$. They were evaluated as catalysts in the ETP process based on cascade reactions: dimerization/isomerization over Ni- AlKIT-6 and metathesis over $\text{WO}_x/\text{KIT-6}$. The catalytic sites have been probed by ammonia temperature-programmed desorption (NH_3 -TPD), hydrogen temperature-programmed reduction (H_2 -TPR), X-photoelectron spectroscopy (XPS) and ^{27}Al MAS NMR.

KIT-6 is a mesoporous material, possessing a bicontinuous cubic structure with $Ia3d$ symmetry and an interpenetrating cylindrical pore system [28]. It is a suitable support for the present catalysts, thanks to its high surface area and large interconnected mesopores, which are key factors for high mass transport properties. As known, these properties are crucial for processes that involve reactive olefins [3, 6].

2. Experimental

2.1. Catalysts preparation

The dimerization/isomerization Ni-AlKIT-6 catalyst has been prepared in three successive steps, as shown in Fig. S1 (ESI). Initially, a pure siliceous material (sample KIT-6) was prepared in water, using (EO)₂₀(PO)₇₀(EO)₂₀ triblock copolymer (Pluronic P123, $M_n = 5\,800\text{ g mol}^{-1}$, Aldrich), tetraethyl orthosilicate (TEOS 99%, Aldrich), HCl 37.5% (Aldrich) and *n*-butanol (99%, Alfa Aesar). The molar ratio of reagents was 1 TEOS/0.017 P123/1.9 HCl/1.3 *n*-butanol/195 H₂O. After stirring for 24 h at 35 °C, the mixture was kept under static conditions at 100 °C for 24 h in an autoclave. The solid was recovered, washed with water, dried at 80 °C and calcined for 8 h in air-flow at 550 °C.

Al-containing material (sample AlKIT-6) was obtained from KIT-6 and sodium aluminate (99%, Carlo Erba) according to the procedure developed by our group [29]. The solid (2 g of Na-AlKIT-6) was then converted into NH₄-AlKIT-6 by ionic exchange (2 h, 30 °C, and 100 mL of 0.5 M NH₄NO₃ aqueous solution). The sample was subjected to nickel-ion exchange with a 0.5 M aqueous solution of Ni(NO₃)₂ obtained from hexahydrate nickel(II) nitrate (98%, Alfa Aesar), following the same procedure as described above. The exchanged sample was dried and then calcined for 5 h in air-flow at 550 °C to achieve the catalyst denoted as Ni-AlKIT-6. A portion of NH₄-AlKIT-6 was calcined for 5 h in airflow at 550 °C to obtain the H-AlKIT-6 sample.

WO_x-based metathesis catalysts, containing 4 and 8 wt% W were prepared by the incipient wetness impregnation method using an aqueous solution of ammonium metatungstate (99%, Honeywell) and KIT-6, Na-AlKIT-6 or H-AlKIT-6 as supports. Before impregnation, the exact amount of water required to fill the support pores was determined. The proper amount of ammonium metatungstate for achieving the requested tungsten loading was dissolved in an appropriate amount of distilled water. This solution was added to the support dropwise. The wet material was dried at 80 °C for at least 6 h and calcined in static air at 550 °C for 8 h. These

materials will be denoted as X-W-KIT-6, X-W-Na-AIKIT-6 and X-W-H-AIKIT-6 (where X = 4 or 8 represents the W loading, wt%).

2.2. Catalysts characterization

The powder XRD measurements were performed on a Bruker AXS D8 diffractometer. The solid textures were evaluated by nitrogen adsorption/desorption at $-196\text{ }^{\circ}\text{C}$, using a Micrometrics ASAP 2020 analyzer. ^{27}Al MAS NMR spectra of the calcinated samples were obtained as previously reported [29] on a Varian 600 MHz WB Premium Shielded spectrometer, equipped with 3.2 mm o.d. ZrO_2 rotors at a rotation speed of 20 kHz. The fresh and spent catalysts were characterized by X-ray photoelectron spectroscopy (XPS). The spent catalyst, carefully recovered from the reactor was kept under a nitrogen atmosphere before characterization. The measurements were performed on an ESCALAB 250 (Thermo Electron) spectrometer equipped with an Al $K\alpha$ source (1486.6 eV), and on a Physical Electronics spectrometer (PHI Versa Probe II Scanning XPS Microprobe with monochromatic X-ray Al $K\alpha$ radiation (100 μm , 100 W, 20 kV, 1486.6 eV) and a dual-beam charge neutralizer. The procedure has been previously described [24].

The acidity of Ni-AIKIT-6 was explored by temperature-programmed desorption (TPD) using ammonia as probe molecule (Micrometrics AUTOCHEM 2910). H_2 -TPR measurements were performed using the same apparatus. The sample (~40 mg) was pre-treated for 6 h in air-flow at $550\text{ }^{\circ}\text{C}$, and then cooled down to room temperature in Ar gas flow. The reduction of the sample was carried out while heating from room temperature to $1100\text{ }^{\circ}\text{C}$ with a ramp of $10\text{ }^{\circ}\text{C min}^{-1}$ using a certified gas mixture of 2 vol% H_2 in Ar (Air Liquide) with a flow rate of 20 mL min^{-1} . Hydrogen concentration at the reactor outlet was measured by thermal conductivity detector (TCD) after removing water by a cooling trap.

Nickel content in the catalyst was measured by atomic absorption spectrometry using a Varian Spectra 220 apparatus and a source emitting monochromatic radiation with a wavelength of 232 nm. The sample (~40 mg) is dissolved in 100 mL of 2 mol L^{-1} sodium hydroxide solution. Tungsten content measurements were performed on a PANanalytical Axios max device with an X-ray source (4 kW rhodium tube). A 100 mg sample was used for analysis.

2.3. Catalytic tests

The performances of the catalysts were evaluated in a laboratory-scale unit (Fig. S2, ESI) equipped with two stainless steel fixed-bed reactors (i.d. = 6 mm, length = 150 mm) coupled in

series. The mass flows of gases were monitored by thermal mass flow control valves (Brooks 5850S HP). Before each test, the catalysts (particle size ranging from 0.15 to 0.25 mm) were activated in-situ for 8 h at 550 °C under a nitrogen gas flow. The catalytic measurements have been realized at constant temperature and pressure, using a feed gas stream consisting of C₂H₄ and N₂ (1:1 v/v). The products have been analyzed online by GC (Varian CP-3800, FID), using a CP-PoraPLOT Q capillary column (25 m, 0.53 mm, 20 μm) and an auto-sampling valve. Ethylene conversion (X) was calculated from the respective concentrations at the inlet (C_i) and outlet (C_o) of the reactor ($X = 1 - C_i / C_o$). Product selectivity for the molecule *i* was $S_i = y/2 \times x_i / \sum x_j$, where *x* stands for mole fraction and *y* is a coefficient equal to C atoms in the respective molecule. The amount of products confined in the catalyst during the tests was evaluated by TGA using a NETZSCH TG 209C apparatus (20 mg catalysts, 20 mL min⁻¹ air, temperature ramp of 10 °C min⁻¹ up to 800 °C).

3. Results and discussion

3.1. Characterisation of catalysts and supports

The powder XRD results showed that all samples prepared in this study were well-organized mesoporous materials. Thus, the small-angle XRD patterns (Fig. S3) showed a diffraction peak d_{211} ($2\theta = 0.97^\circ$) and a peak d_{220} ($2\theta = 1.12^\circ$) characteristic of the cubic *Ia3d* symmetry of KIT-6 materials [28]. No signal was observed in the powder XRD patterns recorded at $2\theta > 5^\circ$, confirming the absence of crystalline NiO or WO_x species (Fig. S4). Additionally, the nitrogen adsorption-desorption isotherms were of type IV, with a sharp capillary condensation step, characteristic of high-quality materials with homogeneous mesopores (Fig. S5, ESI). The main textural properties, calculated from sorption data, as well as the composition and acidity of different samples are summarized in Table 1.

The ²⁷Al MAS NMR spectrum of Ni-AIKIT-6 (Fig. S6, ESI) shows a major signal at about 55 ppm, corresponding to the tetrahedrally-coordinated aluminum species. Such a result confirms that the post-synthesis alumination with sodium aluminate at room temperature is an efficient method to incorporate aluminum into the silica matrix.

Ni-AIKIT-6 had a Si/Al ratio of 11.0 and a Ni content of 2±0.2 wt% (Table 1). The corresponding Ni/Al ratio is 0.25 (mol/mol), indicating an exchange level of NH₄⁺ ions with Ni²⁺ of about 50%. During the calcination at 550 °C (see the experimental section), NH₄⁺ ions are decomposed into ammonia and H⁺, generating the Brønsted acidic sites associated to

aluminum atoms. Note that the acid sites are useful for the 1-butene isomerization in the ETP process [21, 23].

The oxidation state of Ni and Re sites in the catalysts was examined by XPS. The deconvoluted spectrum of the Ni-AIKIT-6 catalyst in the Ni 2*p* region is shown in Fig. 1. The main signal with a binding energy of 857.7 eV is attributed to isolated Ni(II) species [30], and more precisely to tetrahedrally coordinated Ni(II). This result is confirmed by the presence of its primary satellite peak at 863 eV. The weaker signal at 854.2 eV reveals the presence of NiO, which was not detected by XRD because of its small amount. It is commonly accepted that only the isolated Ni species are precursors of the catalytic dimerization/oligomerization sites [29, 30].

Fig. 2 shows the deconvoluted XP spectra of the fresh 4-W-KIT-6 and after reaction (24 h) catalyst samples in the W 4*f* region. Four contributions at 35.0, 36.5, 37.2 and 38.6 eV can be distinguished in the spectra. According to the literature, the doublet W 4*f*_{7/2}-W 4*f*_{5/2} recorded at 35.0 and 37.2 eV can be assigned to W⁵⁺ oxidation state, while the second and more intense doublet at 36.5 and 38.6 eV corresponds to W⁶⁺ [24, 32]. The XPS W 4*f* core level spectrum of the spent catalyst also shows two doublets, but the relative intensity of the doublet at high binding energy assigned to W⁶⁺ is much higher than in the case of the fresh catalyst sample.

The total acidity of W-based catalysts was evaluated by ammonia TPD. As expected, the TPD profiles shown in Fig. 3 and the amount of adsorbed/desorbed ammonia (Table 1) strongly depends on the composition of catalytic materials. Both Al and W generated acid sites when added to the parent KIT-6 silica (4-W-KIT-6, Na-AIKIT-6 and 4-W-Na-AIKIT-6, Fig. 3). For these materials, ammonia desorbed at *T* < 300 °C, which is typical for the weak acid sites. The number and strength of acid sites increased when the sodium ions are replaced by protons (H-AIKIT-6 and 4-W-H-AIKIT-6 samples). The large desorption trace up to 450 °C indicates the presence of medium strength acid sites.

The reducibility of W species has been examined by temperature-programmed reduction with hydrogen (H₂-TPR). The TPR profiles of 4-W-KIT-6, 4-W-Na-AIKIT-6 and 4-W-H-AIKIT-6 revealed a first H₂ consumption signal at ~825 °C and a second one at 1000, 975 and 1025 °C, respectively (Fig. S7, ESI). The two reduction bands can be assigned to the reduction of W⁶⁺ and W⁵⁺ isolated species into metallic W in a two-steps process: W⁶⁺/W⁵⁺ → W⁴⁺ → W⁰ [33,34].

The differences in high-temperature reduction domains could be attributed to the different interactions between W species and the supports.

The absence of bulky WO_3 was demonstrated by X-ray diffraction and H_2 -TPR analyses. The latter analysis showed an interaction between the support and tungsten. W^{6+} and W^{5+} are thus most probably found as isolated WO_x species on the surface of silica. According to the literature [25], two isolated W^{6+} species have been identified. The W^{5+} reflects probably the same species but bearing a hydroxyl (see Scheme 1).

To summarize, all synthesized catalysts are well organized mesoporous materials with high surface area, pore volume and pore diameter of 7.4-8 nm. Ni-AIKIT-6 contains Ni^{2+} and H^+ sites, while metathesis catalysts contain W^{6+} and W^{5+} -species.

3.2. ETP on Ni-W catalysts

In order to produce propylene from ethylene, two catalytic beds consisting of Ni-AIKIT-6 and W-based materials were placed in two consecutive reactors. The dimerization/isomerization reactions occurred in the first reactor in the presence of 0.2 g of Ni-AIKIT-6 operated at 60 °C and 3 MPa. The feed consisted of 2 L h⁻¹ of ethylene-nitrogen mixture (1/1, v/v). The choice of these parameters was based on our previous studies [21,29,31] and dimerization experiments performed over Ni-AIKIT-6 (results are shown in ESI).

The complete effluent gas stream from the first reactor, containing the unreacted ethylene and the oligomers (mainly butenes) was directed to the second reactor, where the metathesis step occurs. The second reactor contained 0.5 g of W-based catalyst and was operated at 450 °C and 0.1 MPa. In the first reactor over Ni-AIKIT-6, ethylene was mainly converted to butenes. Coupling the two reactors, the main product was propylene, but some amounts of pentenes and heptenes were formed. These results indicate that the W-based catalyst also is able to catalyze metathesis reactions involving olefins higher than C₄. Typical chromatograms obtained in the ethylene dimerization over Ni-AIKIT-6, and dimerization-metathesis over Ni-AIKIT-6 + 4-W-KIT-6 are given in Fig. S8 (ESI).

3.2.1. Effect of support and W loading

4-W-KIT-6, 4-W-Na-AIKIT-6 and 4-W-H-AIKIT-6 metathesis catalysts with 4 wt % W have been coupled with Ni-AIKIT-6 to perform the ETP reactions. Table 2 summarizes the most relevant results in terms of product distribution obtained at a similar overall ethylene conversion

of ~50%. For these tests, ethylene conversion in the first reactor was about 35%. The results obtained on a catalytic system containing 8 wt % W (8-W-KIT-6) are also included in Table 2.

The effect of support on the amount of each ETP product is noticeable. First, the amount of propylene (which is the main product for all catalytic systems) decreased from 59.4% over the 4-W-KIT-6 catalyst with an Al-free support to 44.0 and 36.1% over the 4-W-Na-AIKIT-6 and 4-W-H-AIKIT-6 catalysts, respectively. On the other hand, the concentration of the C₄₊ hydrocarbons increased in the opposite way for the three catalysts. The selectivity in (C₃ + C₄) hydrocarbons considered as useful products in the ETP process, was very high for all catalysts, but some differences are apparent. For example, 85, 79.8 and 66.7% selectivity was obtained over 4-W-KIT-6, 4-W-Na-AIKIT-6 and 4-W-H-AIKIT-6, respectively. Additionally, the 1-C₄/2-C₄ ratio in butenes significantly decreased (Table 2). In our opinion, the acidity of the catalyst supports can be considered as the main parameter responsible for these differences. First, the WO_x species catalyse the metathesis reactions between butenes and ethylene (Scheme 2). However, at 450 °C, the acid sites of the alumina-based metathesis catalysts (i.e. 4-W-Na-AIKIT-6 and 4-W-H-AIKIT-6) can activate a series of undesirable reactions, e.g. oligomerization, isomerization, and cracking which involve the primary products (propylene, 1-butene).

To conclude, in the ETP process carried out under the present conditions and with metathesis catalysts based on KIT-6 materials, a non-acid pure silica is more efficient as support than the silica-alumina supports. According to Le Roux *et al.* [35], the acidity of the support improved the self-metathesis of propylene with a tungsten catalyst. In our study, this effect is manifested by an over-activity of the most acidic catalyst leading to a decrease of propylene selectivity.

To establish the role of W loading, the ETP process has been carried out in the presence of Ni-AIKIT-6 and 8-W-KIT-6 catalysts. By comparing the catalysts with 4 and 8% W (Table 2), it can be seen that the product distribution depends on the W amount in the catalyst. Thus, the amount of propylene and useful molecules (C₃ + C₄) is decreased when W loading increased from 4 to 8%, and that in favour of the heavier molecules. These results suggest that at a higher concentration of W sites, the catalyst exhibits an over activity in metathesis, and thus the C₃ and 1-C₄ primary products are consumed in subsequent reactions with other olefins. This means that a perfect balance between the amount of Ni and W sites in the ETP process is required to efficiently convert ethylene to propylene.

3.2.2. Evaluation of catalyst deactivation

The stability against deactivation of the 4-W-KIT-6 metathesis catalyst was examined in a long-term (24 h on reaction stream) catalytic test. To increase the total ethylene conversion, the first reactor containing the Ni-Al-KIT-6 catalyst was operated at 120 °C and 3 MPa. To ensure a quantity of ethylene sufficient for the metathesis reaction in the second reactor, the conversion of ethylene in the first reactor was kept ~50%. The ethylene conversion, as well as the amount of C₃ and C₄ among the ETP products as a function of time on stream are given in Fig. 4.

The initial conversion of ethylene was 72%, but it increased during the first 4 h to reach a plateau at ~85%. The molar selectivity to propylene decreased progressively. A 65% initial selectivity is noticed which drops to 51% after 5 h on reaction stream, and then remains stable. The selectivity to butenes remains constant at ~27% during 24 h on reaction stream. The average concentration in C₅, C₆, C₇ and C₈ was 9, 4, 3 and 1 vol%, respectively. The yield in propylene (ethylene conversion x propylene selectivity) corresponding to the plateau was ~45%, while the productivity in propylene was 39 mmol g⁻¹ h⁻¹.

To check whether the catalysts suffered from any modification after 24 h on reaction stream, these were analysed by powder XRD, TGA and XPS. The analysis of the catalysts diffractograms before and after reaction (Fig. S9) indicates no major structural deterioration of the KIT-6 support after deposition of nickel and tungsten metals. The TGA profiles of the spent nickel-based catalyst showed a weight loss of 55% (Fig. S10, ESI). The signal derivative shows three distinctive mass-loss peaks centered at ~275, 330 and 500 °C. The relatively large mass loss on this catalyst is related to its dimerization role. Heavier products formed by oligomerization can be trapped in the pores and this confirms the need of using a support with an adequate pore size and pore volume. The TGA profile of the spent tungsten catalyst showed a weight loss of about 25% between 450 and 500 °C, proving that under the present reaction conditions, only a small amount of heavy carbonaceous species were adsorbed on the metathesis catalyst. The XP spectra of the fresh and used Ni-Al-KIT-6 and 4-W-KIT-6 catalysts are given in Fig. 1 and Fig. 2, respectively. The XP spectrum of the nickel catalyst after reaction shows little change in the surface composition of nickel species (Fig. 1). The tetrahedrally coordinated Ni(II) species are still the majority species. However, the 854.2 eV signal (highlighting the presence of NiO species) is higher on the spent than the fresh catalyst. Thus, there is degradation of a small part of nickel sites.

As for the fresh sample, W⁶⁺ and W⁵⁺ species are still present on the spent catalyst (Fig. 2), but their ratio (W⁶⁺/W⁵⁺) appears increased compared to that before the reaction, ca. 61-39

(at.%) before the reaction to ca. 82-18 (at%) after the reaction. We have shown that W^{6+} can represent isolated WO_x sites on the surface of the solid and W^{5+} might represent the same species but with hydroxyl attached (Scheme 1). This decrease in the amount of W^{5+} can thus reflect a decrease in the hydroxyl concentration on the surface of the tungsten-based catalyst. It is speculated that the proportion of hydroxyl might be reduced during activation under air prior to the reaction.

3.2.3. Comparison with the literature

As stated in the Introduction section, various catalytic systems and procedures were used for converting ethylene into propylene without adding other hydrocarbons in the process. Inhomogeneous results were obtained, depending on the catalyst (see Table S1, ESI). Over Ni-MCM-41 and Ni-MCM-48 catalysts, the specific activity in propylene was 0.8-3.1 $\text{mmol g}_{\text{catal}}^{-1} \text{h}^{-1}$ at 350-400 °C [13-15]. Using W-H₃/γ-Al₂O₃, Taoufik et al. [17] obtained 9.6 $\text{mmol g}_{\text{catal}}^{-1} \text{h}^{-1}$ at 150 °C. Over polymetallic NiSO₄/Re₂O₇/γ-Al₂O₃ [13] and MeO/Re₂O₇/B₂O₃-Al₂O₃ (Me = Pd or Ni) [19] catalysts, the specific activity of propylene was 12.6 and 2.8 $\text{mmol g}_{\text{catal}}^{-1} \text{h}^{-1}$, respectively. The best results were obtained by combining two distinct dimerization/metathesis catalysts in a single reactor: 48 $\text{mmol g}_{\text{catal}}^{-1} \text{h}^{-1}$ over Ni-AISBA-15 + MoO₃-SiO₂-Al₂O₃ [21], 28 $\text{mmol g}_{\text{catal}}^{-1} \text{h}^{-1}$ over Ni-AlSiO₂ + MoO_x/(Al)SiO₂ [22], and 26 $\text{mmol g}_{\text{catal}}^{-1} \text{h}^{-1}$ over Ni-AIKIT-6 + ReO_x/γ-Al₂O₃ [23]. In this study, using two catalysts (Ni-AIKIT-6 + WO_x/KIT-6) and two reactors, we were also able to obtain a high ethylene productivity, i.e. 40 $\text{mmol g}_{\text{catal}}^{-1} \text{h}^{-1}$. Moreover, these catalysts showed very high stability against deactivation (Fig. 4). Note that the catalytic systems previously evaluated in all ETP processes suffered from significant deactivation [13-23]. Fig. 5 compares the yield in propylene vs. time on stream for the dual catalytic system, Ni-AIKIT-6 + 4-W-KIT-6 with the yields obtained over Ni-AISBA-15 + MoO₃-SiO₂-Al₂O₃ [21] and Ni-AIKIT-6 + ReO_x/γ-Al₂O₃ dual catalytic systems reported [23]. Undoubtedly, the W-based catalytic system is more efficient and much more stable than the other ones.

The direct conversion of ethylene to propylene has been investigated using two dual catalytic systems and two reactors in series. The cascade reactions involved in the process, i.e. dimerization/isomerization/metathesis were catalyzed by Ni²⁺, H⁺ (both delivered by Ni-AIKIT-6 catalyst) and W (from WO_x/KIT-6 catalyst), respectively. Even if the ETP process was governed by the metathesis step, a perfect balance between the amount of Ni and W sites

is essential to efficiently convert ethylene to propylene. For the W-based metathesis catalysts, the support consisting of a non-acid pure KIT-6 silica was more efficient than the silica-alumina supports. Unlike catalytic systems based on MoO_x and ReO_x , those based on WO_x were highly active and stable over a long reaction period. Thus, the ethylene conversion ($\sim 85\%$), as well as the yield in propylene (45%) remained unchanged during 24 h on reaction stream.

The encouraging results obtained in the present work about the catalytic conversion of ethylene into propylene could create the basis for new research focused on the conversion of non-oil-based sources into low-carbon olefins. Thus, the ETP process could be incorporated as a second stage into an integrated system, including the bio-ethanol dehydration to ethylene and its conversion into propylene.

Acknowledgments

ERC thanks for financial support project RTI2013-099668-BC22 of Ministerio de Ciencia, Innovación y Universidades and FEDER.

Credit author statement

Remi Beucher: Investigation, Writing- Original draft preparation; **Claudia Cammarano:** Writing- Reviewing and Editing, Validation; **Enrique Rodríguez-Castellón:** Investigation, Validation; **Vasile Hulea:** Conceptualization, Writing- Reviewing and Editing, Supervision

Declaration of interests

The authors declare that they have no known competing financial interests or personal relationships that could have appeared to influence the work reported in this paper.

Supplementary data

Supplementary material**References**

- [1] A.V. Lavrenov, L.F. Saifulina, E.A. Buluchevskii, E.N. Bogdanets, Propylene production technology: Today and tomorrow, *Catal. Ind.* 7 (2015) 175–187.
- [2] P. Tian, Y. Wei, M. Ye, Z. Liu, Methanol to olefins (MTO): From fundamentals to commercialization, *ACS Catal.* 5 (2015) 1922–1938.
- [3] V. Hulea, Toward platform chemicals from bio-based ethylene. Heterogeneous catalysts and processes, *ACS Catal.* 8 (2018) 3263–3279.
- [4] M. Ghashghaee, Heterogeneous catalysts for gas-phase conversion of ethylene to higher olefins, *Rev. Chem. Eng.* 34 (2018) 595-655.
- [5] V. Blay, E. Epelde, R. Miravalles, L. Alvarado Perea, Converting olefins to propene: Ethene to propene and olefin cracking *Catal. Rev.* 60 (2018) 278-335.
- [6] V. Hulea, Direct Transformation of butenes or ethylene into propylene by cascade catalytic reactions, *Catal. Sci. Technol.* 9 (2019) 4466-4477.
- [7] J. Sun, Y. Wang, *ACS Catal.* Recent advances in catalytic conversion of ethanol to chemicals, 4 (2014) 1078-1099.
- [8] M. Zhang, Y. Yu, Dehydration of ethanol to ethylene, bioethylene production from ethanol: A review and techno-economical evaluation, *Ind. Eng. Chem. Res.* 52 (2013) 9505-9514.
- [9] A. Mohsenzadeh, A. Zamani, M.J. Taherzadeh, Bioethylene production from 1st and 2nd generation ethanol: A mini review and techno-economical evaluation, *ChemBioEng Rev.* 4 (2017) 1-18.
- [10] H. Oikawa, Y. Shibata, K. Inazu, Y. Iwase, K. Murai, S. Hyodo, G. Kobayashi, T. Baba, Highly selective conversion of ethene to propene over SAPO-34 as a solid acid catalyst, *Appl. Catal. A: Gen.* 312 (2006) 181-185.

- [11] W. Dai, X. Sun, B. Tan, G. Wu, L. Li, N. Guan, M. Hunger, Verifying the mechanism of the ethene-to-propene conversion on zeolite H-SSZ-13, *J. Catal.* 314 (2014) 10-20.
- [12] J. W. Jun, N.A. Khan, P.W. Seo, C.U. Kim, S.H. Jung, Conversion of Y into SSZ-13 zeolites and ethylene-to-propylene reactions over the obtained SSZ-13 zeolites, *Chem. Eng. J.* 303 (2016) 667-674.
- [13] M. Iwamoto, Y. Kosugi, Selective conversion of ethylene to propene and butenes on nickel ion-loaded mesoporous silica catalysts, *J. Phys. Chem. C.* 111 (2007) 13-15.
- [14] A. Frey, O. Hinrichsen, Comparison of differently synthesis Ni(Al)MCM-48 catalysts in the ethene to propene reaction, *Microporous Mesoporous Mater.* 164 (2012) 164-171.
- [15] L.A. Perea, T. Wolff, P. Veit, L. Hilfert, F.T. Edelmann, C. Hänel, A. Seidel-Morgenstern, Alumino-mesostructured Ni catalyst for the direct conversion of ethene to propene, *J. Catal.* 305 (2013) 154-168.
- [16] M. Stoyanova, U. Bentrup, H. Atia, E.V. Kondratenko, D. Linke, U. Rodemerck, The role of speciation of Ni²⁺ and its interaction with the support for selectivity and stability in the conversion of ethylene to propene, *Catal. Sci. Technol.* 9 (2019) 3137-3148.
- [17] M. Taoufik, E. Le Roux, J. Thivolle-Cazat, J.M. Basset, Direct transformation of ethylene into propylene catalyzed by a tungsten hydride supported on alumina: Trifunctional single-site catalysis, *Angew. Chem., Int. Ed.* 46 (2007) 7202-7205.
- [18] L. Li, R.D. Palcheva, K.M. Jens, Conversion of ethene to propene by a dual function NiSO₄/Re₂O₇/γ-Al₂O₃ catalyst, *Appl. Catal.* 56 (2013) 783-788.
- [19] E.A. Buluchevskii, M.S. Mikhailova, A.V. Lavrenov, One-stage synthesis of propylene from ethylene using Pd-Re₂O₇/B₂O₃-Al₂O₃ catalyst, *Chem. Sustainable Dev.* 21 (2013) 47-51.
- [20] M. Ghashghaee, V. Farzaneh, Nanostructured hydrotalcite-supported RuBaK catalyst for direct conversion of ethylene to propylene, *Russ. J. Appl. Chem.* 91 (2018) 972-976.
- [21] R.D. Andrei, M.I. Popa, F. Fajula, C. Cammarano, A. Al Khudhair, K. Bouchmella, H. Mutin, V. Hulea, Ethylene to propylene by one-pot catalytic cascade reactions, *ACS Catal.* 5 (2015) 2774-2777.
- [22] R.D. Andrei, M.I. Popa, C. Cammarano, V. Hulea, Nickel and molybdenum containing mesoporous catalysts for ethylene oligomerization and metathesis, *New J. Chem.* 40 (2016) 4146-4152.

- [23] R. Beucher, R.D. Andrei, C. Cammarano, A. Galarneau, F. Fajula, V. Hulea, Selective production of propylene and 1-butene from ethylene by catalytic cascade reactions, *ACS Catal.* 8 (2018) 3636-3640.
- [24] R. Beucher, C. Cammarano, E. Rodríguez-Castellón, V. Hulea, Direct transformation of ethylene to propylene by cascade catalytic reactions under very mild conditions, *Ind. Eng. Chem. Res.* 59 (2020) 7438–7446.
- [25] S. Lwin, I.E. Wachs, Olefin metathesis by supported metal oxide catalysts, *ACS Catal.* 4 (2014) 2505–2520.
- [26] J.C. Mol, Industrial applications of olefin metathesis, *J. Mol. Catal. A.: Chem.* 213 (2004) 39–45.
- [27] S. Lwin, Y. Li, A.I. Frenkel, I.E. Wachs, Nature of WO_x sites on SiO_2 and their molecular structure–reactivity/selectivity relationships for propylene metathesis, *ACS Catal.* 6 (2016) 3061–3071.
- [28] F. Kleitz, S.H. Choi, R. Ryoo, Cubic and large mesoporous silica: synthesis and replication to platinum nanowires, carbon nanorods and carbon nanotubes, *Chem. Commun.* (2003) 2136-2137.
- [29] R.D. Andrei, M.I. Popa, F. Fajula, V. Hulea, Heterogeneous oligomerization of ethylene over highly active and stable Ni-ASBA-15 mesoporous catalysts, *J. Catal.* 323 (2015) 76-84.
- [30] S. Moussa, P. Concepción, M.A. Arribas, A. Martínez, Nature of active nickel sites and initiation mechanism for ethylene oligomerization on heterogeneous Ni-beta catalysts, *ACS Catal.* 8 (2018) 3903-3912.
- [31] M. Lallemand, A. Finiels, F. Fajula, V. Hulea, Continuous stirred tank reactor for ethylene oligomerization catalyzed by NiMCM-41, *Chem. Eng. J.* 172 (2011) 1078-1082.
- [32] M. Seifollahi Bazarjani, M. Hojamberdiev, K. Morita, G. Zhu, G. Cherkashinin, C. Fasel, T. Herrmann, H. Breitzke, A. Gurlo, R. Riedel, Visible light photocatalysis with $\text{c-WO}_3 \cdot x\text{H}_2\text{O}$ nanoheterostructures in situ formed in mesoporous polycarbosilane-siloxane polymer, *J. Am. Chem. Soc.* 135 (2013) 4467-4475.

[33] D. Vermaire, P. Van Berge, The preparation of WO_3TiO_2 and $\text{WO}_3\text{Al}_2\text{O}_3$ and characterization by temperature-programmed reduction, *J. Catal.* 116 (1989) 309-317.

[34] R. Kourieh, S. Bennici, M. Marzo, A. Gervasini, A. Auroux, Investigation of the WO_3/ZrO_2 surface acidic properties for the aqueous hydrolysis of cellobiose, *Catal. Commun.* 19 (2012) 119-126.

[35] E. Le Roux, M. Taoufik, A. Baudouin, C. Copéret, J. Thivolle-Cazat, J.M. Basset, B.M. Maunders, G.J. Sunley, Silica-alumina-supported, tungsten-based heterogeneous alkane metathesis catalyst: Is it closer to a silica- or an alumina-supported system?, *Adv. Synth. Catal.* 349 (2007) 231-37.

Fig. 1. Ni $2p_{3/2}$ X-ray photoelectron spectra recorded on Ni-AlKIT-6 sample before (fresh) and after 24 h of reaction (aged).

Fig. 2. W $4f$ X-ray photoelectron spectra of 4-W-KIT-6 sample before (fresh) and after 24 h of reaction (aged).

Fig. 3. Ammonia TPD profiles of the supports alone and the various catalysts.

Fig. 4. Ethylene conversion (\circ), C_3 (\square) and C_4 (\diamond) selectivity vs. time on reaction stream. Reaction conditions: Feed = 2 L h^{-1} of ethylene-nitrogen mixture (1/1, v/v); Dimerization reactor: Ni-AlKIT-6 (0.5 g), $T = 120^\circ\text{C}$, $P = 3.0\text{ MPa}$; Metathesis reactor: 4-W-KIT-6 (0.5 g), $T = 450^\circ\text{C}$, $P = 0.1\text{ MPa}$.

Fig. 5. Yields in propylene over (\square) Ni-Mo dual catalytic system - ref. 21, (Δ) Ni-Re dual catalytic system - ref. 23, and (\bullet) Ni-W catalysts - this study ; Yield = ethylene conversion x selectivity in propylene. Ni-Mo and Ni-Re dual catalytic systems were evaluated in a single fixed-bed reactor at 3.0 MPa and 80°C or 60°C , respectively.

Scheme 1. Isolated sites of W^{6+} and W^{5+} species on the surface of the metathesis catalysts.

Scheme 2. Primary metathesis reactions between ethylene and n -butenes.

Table 1. Composition, textural properties and surface acidity of catalysts.

Sample	Si/Al (mol mol ⁻¹)	Me ^a (wt %)	D _p ^b (nm)	V _p ^b (mL g ⁻¹)	S _{BET} ^b (m ² g ⁻¹)	Acidity ^c (mmol NH ₃ g ⁻¹)
Ni-AlKIT-6	11.0±0.2	2±0.2	7.3	0.73	440	0.20
4-W-KIT-6	-	4.5±0.1	8.1	0.95	370	0.10
4-W-Na-AlKIT-6	11.0±0.2	4.6±0.1	7.4	0.71	420	0.18
4-W-H-AlKIT-6	11.0±0.2	4.5±0.1	7.4	0.67	400	0.32

^a Me = Ni or W, ^b BdB pore diameter (D_p), total pore volume (V_p), ^c BET specific surface area (S_{BET}).
^c from NH₃-TPD.

Table 2. Ethylene conversion and product distribution in the ETP process: effect of support used in the metathesis catalysts^a.

Metathesis catalyst	C ₂ conv. ^b (%)	Product distribution ^a (%mol)						C ₄ isomers ^b (%)	
		C ₃	C ₄	C ₅	C ₆	C ₇	C ₈	1-C ₄	2-C ₄
4-W-KIT-6	48.8	59.4	25.6	8.0	3.1	1.7	2.0	81.1	18.9
4-W-Na-Al-KIT-6	50.4	44.5	35.8	7.0	8.5	1.2	3.5	57.7	42.3
4-W-H-Al-KIT-6	56.2	36.1	30.6	10.4	16.0	4.5	2.3	41.6	58.4
8-W-KIT-6	48.0	44.2	32.8	5.0	7.8	3.5	6.5	65.4	34.6

^a Reaction conditions: Feed = 2 L h⁻¹ of ethylene-nitrogen mixture (1/1, v/v); First reactor: 0.2 g of Ni-AlKIT-6, 60 °C, 3 MPa; Second reactor: 0.5 g of W-based catalyst, 450 °C, 0.1 MPa; ^b after the second reactor.

Graphical abstract

Highlights

- This is an efficient catalytic way for converting ethylene to propylene (ETP)
- The ETP process is conducted in cascade mode, using two catalysts
- In the first reactor, over Ni-AIKIT-6, ethylene is selectively converted into *n*-C4
- In the second one, over WO_x/KIT-6, the unconverted ethylene with the formed *n*-C4 will generate propylene
- Both catalysts are highly active and stable in the ETP process

Journal Pre-proof

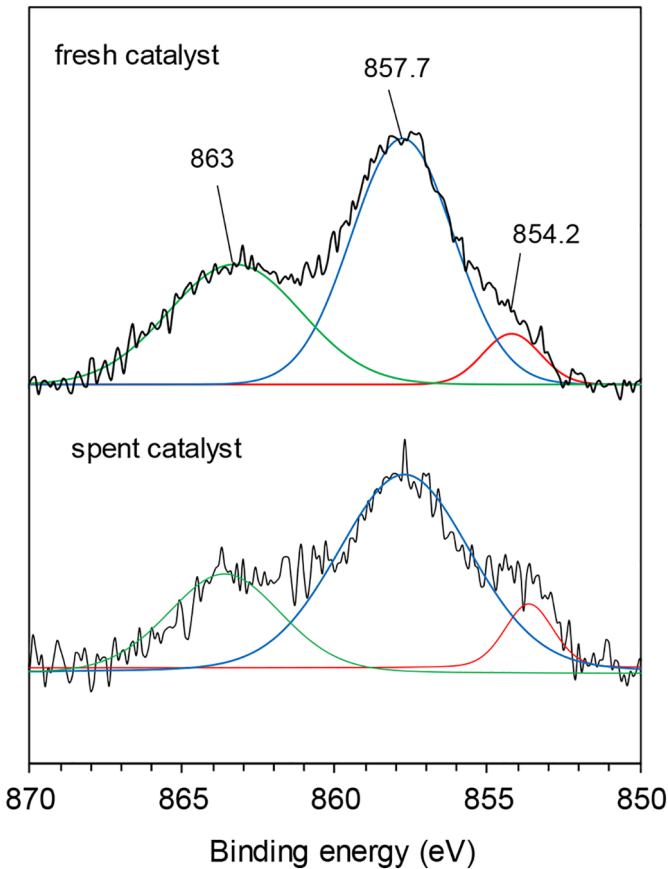


Figure 1

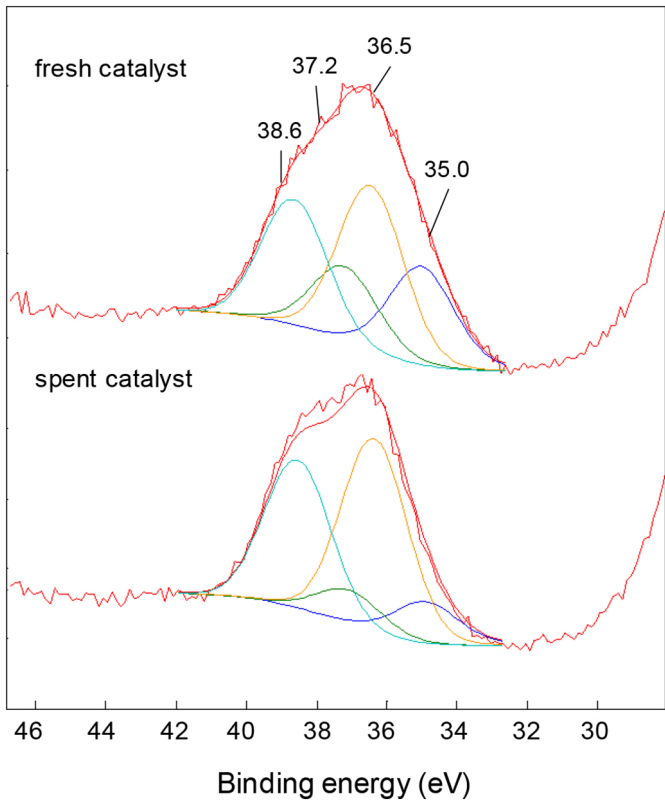


Figure 2

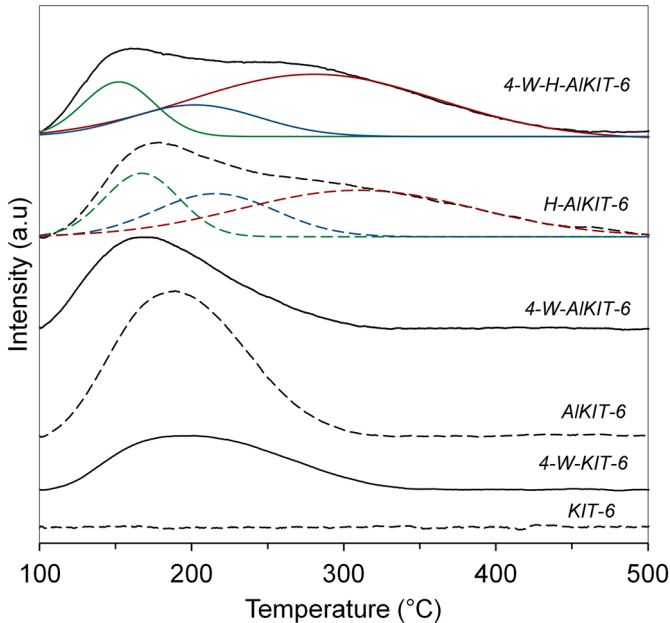


Figure 3

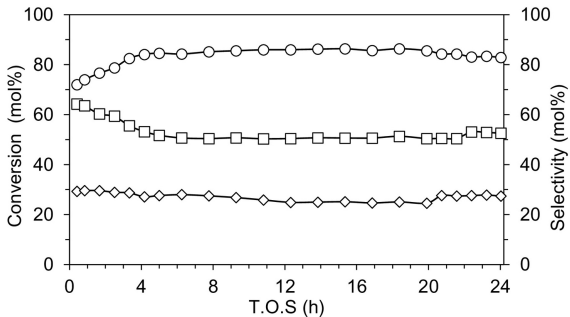


Figure 4

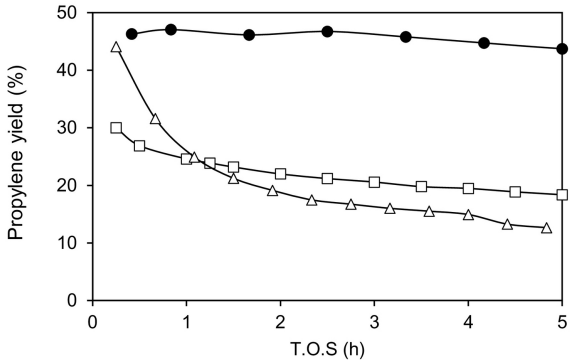


Figure 5